Cardiovasc Intervent Radiol (2017) 40:1609–1616
DOI 10.1007/s00270-017-1689-y

LABORATORY INVESTIGATION

Microwave Ablation of the Lung in a Porcine Model: Vessel Diameter Predicts Pulmonary Artery Occlusion

George A. Carberry[1] · Elisabetta Nocerino[1] · Mircea M. Cristescu[1] · Amanda R. Smolock[1] · Fred T. Lee Jr.[2] · Christopher L. Brace[2]

Received: 15 February 2017 / Accepted: 3 May 2017 / Published online: 11 May 2017

Abstract
Purpose To determine the size of pulmonary artery (PA) at risk for occlusion during percutaneous microwave ablation and to assess the effect of vessel diameter, number, and patency, on ablation zone volume.
Materials and Methods Computed tomography (CT) fluoroscopy-guided percutaneous microwave ablations were performed in 8 pigs under general anesthesia. All ablations were performed at 65 W for 5 min with a single 17-gauge antenna positioned in the central third of the lungs. A CT pulmonary angiogram was performed immediately after the ablations. The maximum diameter, number and patency of PA branches within each ablation zone were recorded. Ablation volumes were measured at gross dissection and with CT. Student's *t* test was used to compare ablation zone volumes among groups.
Results Twenty-one pulmonary ablations were performed. Six of the ablation zones (29%) contained at least 1 occluded PA branch. The mean diameter of the occluded PA branches in the ablation zones (2.4 mm; range, 2.0–2.8 mm) was significantly smaller than non-occluded PA branches (3.7 mm; range: 2.1–6.9 mm; $p = 0.009$). No PA branches ≥3 mm in size were occluded. There was no significant difference in volume of gross ablation zones that contained occluded versus non-occluded PAs ($p = 0.42$), one versus multiple PAs ($p = 0.71$), or PAs <3 mm versus ≥3 mm in diameter ($p = 0.44$).
Conclusions PAs ≥3 mm in size have a low risk for iatrogenic occlusion during percutaneous microwave ablation. The presence of multiple adjacent PA branches, an occluded PA branch, and a vessel diameter ≥3 mm within the ablation zone had no observed effect on ablation zone volume.

Keywords Microwave ablation · Percutaneous ablation · Lung neoplasm · Pulmonary artery

Introduction

For patients with primary and secondary lung malignancies that are medically unfit for surgical resection, percutaneous thermal ablation is an effective therapeutic option that is associated with low procedural morbidity [1–3]. Maintaining its favorable risk-benefit profile requires a balance of treatment effectiveness and safety to ensure complete tumor eradication while also preventing iatrogenic vascular injury, which can manifest as vessel thrombosis, intraparenchymal hemorrhage or massive hemoptysis [4–6].

Convection of local ablation temperatures ("heat sink") from both ventilation and blood flow plays an important role in this balance of effectiveness and safety during pulmonary ablations [7–9]. While vascular heat sink contributes to local tumor recurrence by limiting tumoricidal temperatures at the periphery of the ablation zone, it simultaneously prevents endothelial damage and large vessel injury. Prior clinical studies have shown that tumors are more likely to recur around large heat sinks such as the heart and aorta [10] and that proximity to large blood

The results of this study were presented at the WCIO meeting in Boston in 2016.

✉ George A. Carberry
gcarberry@uwhealth.org

[1] Department of Radiology, University of Wisconsin–Madison, 600 Highland Ave., Madison, WI 53792, USA

[2] Department of Radiology and Biomedical Engineering, University of Wisconsin–Madison, 600 Highland Ave., Madison, WI 53792, USA

vessels and bronchi limits the primary and secondary effectiveness of radiofrequency tumor ablation [11]. These observations are confirmed by an experimental animal study using radiofrequency ablation which quantified blood vessel diameter based on risk of injury and found that vessels >3 mm in size have a low risk of vascular injury in the lung that decreases as vessel diameter increases [12]. Vascular convection has also been shown to represent an independent risk factor for local tumor progression during cryoablation [13].

Unlike radiofrequency ablation, microwave ablation is not negatively impacted by the reduced electrical conductivity of aerated lung and as a result, produces larger pulmonary ablation zones [14, 15]. In the liver [16, 17], kidney [18] and lung [14, 19], microwave has also proven less susceptible to vascular heat sink, likely related to a larger zone of direct heating, making it an increasingly utilized modality for lung ablation. One animal study demonstrated a higher percentage of small vessel (<2 mm) occlusion with microwave ablation compared to radiofrequency ablation [19]. However, no prior studies have determined the size of larger vessels in the lung at risk for occlusion with microwave ablation. These data would guide antenna placement during pulmonary microwave ablation, allowing more complete ablation zone coverage of perivascular tumors to reduce incidence of local progression while preventing large vessel occlusion.

Therefore, the primary objective of the study was to determine the size of a pulmonary artery at risk for occlusion during pulmonary microwave ablation. Because of the proven effect of vascular convection in the lung, secondary objectives were to determine the effect of vessel size, patency, and presence of multiple adjacent pulmonary artery branches on the resultant ablation zone size.

Materials and Methods

Animal Care Protocol

This study was performed under approval from our institutional animal care and use committee and complied with National Research Council guidelines [20]. Eight female swine (mean weight = 70 kg; Arlington Farms, Arlington, Wisconsin) were sedated with tiletamine hydrochloride and zolazepam hydrochloride (Telazol; Fort Dodge Animal Health, Fort Dodge, Iowa), atropine (Phoenix Pharmaceutical, St. Joseph, Missouri) and xylazine hydrochloride (Xyla-Ject; Phoenix Pharmaceutical, St Joseph, Missouri) administered by intramuscular injection. The animals were intubated, administered isoflurane anesthetic (Halocarbon Laboratories, River Edge, New Jersey), and mechanically ventilated. An ear vein was cannulated with a 20-gauge angiocatheter through which intravenous fluids were administered.

Experimental Setup

Each animal was positioned supine on the computed tomography (CT) table (GE LightSpeed, Milwaukee, WI). A pre-ablation CT pulmonary angiogram was performed utilizing a standard pulmonary embolism protocol (1.25 mm slice thickness, 0.625 interval, Smart mA, 120 kVP, 100 mL iohexol 300 with 10 mL saline chase, 5 ml/sec via Smart Prep). Percutaneous pulmonary ablations were then carried out with a single 17-gauge gas-cooled microwave antenna (15 cm PR probe, Certus 140 generator, NeuWave Medical, Inc., Madison, WI) that was placed under CT-fluoroscopic guidance (2.5 mm collimation; 0.5 s rotation time; 40 mA). Each antenna was randomized to either the right or left lung and placed near large pulmonary vessels in the central third of the lung. A maximum of three antennas were placed in each animal to avoid overlapping ablations; in 3 animals only 2 ablations were performed. The ablations were performed sequentially at 65 W generator output for 5 min.

Following the ablations, an unenhanced chest CT scan (1.25 mm slice thickness, 0.625 mm interval, Smart mA, 120 kVp) was performed with the antennas in place to facilitate ablation zone measurements along the axis of the antenna shaft with the use of multiplanar image reconstructions. The antennas were then removed, and a repeat CT pulmonary angiogram was performed using the same parameters as the pre-ablation CT pulmonary angiogram.

Gross Tissue Preparation

The animals were sacrificed after the second pulmonary CT angiogram with an intravenous injection of Beuthanasia-D (390 mg/mL pentobarbital sodium and 40 mg/mL phenytoin sodium at 0.2 mL/kg; Schering-Plough, Kenilworth, New Jersey) 3 h after the last ablation in order to allow normal histologic changes of pulmonary necrosis to develop prior to examination. The lungs were removed en bloc. A blunt 17-gauge needle stylet was used to cannulate the existing microwave antenna tract in the lung tissue, and the pulmonary ablations were sliced down the axis of the stylet shaft. The two halves of the ablation zones were digitally photographed on a flatbed high-resolution scanner adjacent to a ruler.

CT Evaluation and Measurements

Two investigators (GC and EN) evaluated the CT pulmonary angiograms and collected the following data in consensus. The pre-ablation CT pulmonary angiogram

images were evaluated to confirm the absence of a preexisting pulmonary artery occlusion. The immediate post-ablation unenhanced CT scan with the antennas in place was reformatted into multiple oblique planes along the axis of the antenna shaft on a PACS workstation (McKesson Medical, San Francisco, CA) to measure the length and diameter of the pulmonary ablation zones as delineated by the area of ground glass opacity [21, 22] (Fig. 1A, B). The volume of each ablation zone was calculated using an ellipsoid assumption ($\pi \cdot L \cdot D^2/6$, where L is length, and D is diameter) and recorded.

The post-ablation CT pulmonary angiogram was used to identify the number of separate pulmonary artery branches within each ground glass ablation zone, excluding branches with maximum diameters less than 2 mm in size, as measured from vessel outer wall to outer wall with digital calipers. The patency of the pulmonary arteries within each ablation zone was then assessed. If an ablation zone contained an occluded pulmonary artery, the maximum diameter of the vessel, measured at the most proximal end of the occluded segment, was recorded (Fig. 2A).

The distance from the emission point of the antenna (a point 1 cm proximal to the tip) to all pulmonary arteries measuring <3 mm in maximum diameter was calculated using the Pythagorean Theorem ($a^2 + b^2 = c^2$) as follows. The distance along the *craniocaudal* axis between the vessel and the emission point was calculated using the difference in table position between the two points on the transverse CT images (a^2). Next, the distance along the *transverse* plane from the same point on the craniocaudal axis to the emission point was recorded (b^2). Therefore, the hypotenuse of the triangle (c^2) represented the closest distance between the vessel and emission point (Fig. 3). For the occluded vessels, the measurement was made from the most proximally occluded aspect of the vessel to the emission point; for the non-occluded vessels, it was made from the largest diameter of the vessel in the ablation zone.

The CT pulmonary angiogram was also evaluated for the presence of (a) pulmonary artery occlusion remote from the ablation zone, (b) a peripheral wedge-shaped opacity indicative of pulmonary infarct, (c) an acute pulmonary artery pseudoaneurysm and d) large intraparenchymal hemorrhage (≥2 lung segments).

Gross Pathology Measurements

The length and maximum diameter of the pulmonary ablation zones were digitally measured, and the volume of each ablation zone was calculated using an ellipsoid assumption, as described for the CT measurements above (Fig. 1C). Gross tissue measurements included the outer edge of the transition zone [14].

Statistical Analysis

A two-tailed student's t test (R software, version 3.0.I, R Foundation for Statistical Computing, Vienne, Austria) was used to compare the maximum diameter of the occluded versus non-occluded pulmonary arteries and to compare the CT diameter and gross volume of the gross ablation zones which contained occluded versus non-occluded pulmonary arteries, those ablation zones that contained one

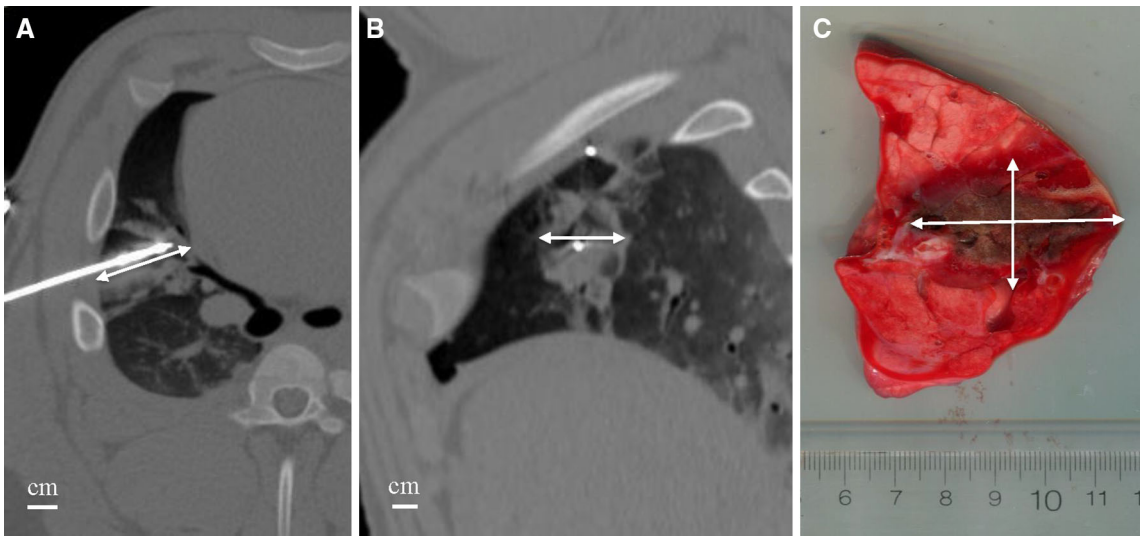

Fig. 1 CT and gross pathology measurement techniques. Multiplanar reconstructions generated along the axis of the microwave antenna provided the total ablation zone length (**A**, *arrow*) and diameter (**B**, *arrow*) based upon the pulmonary ground glass opacity following ablation. The length and diameter of the ablation zone were also measured with gross evaluation (**C**). The volume of the ablation zones at CT and gross analysis was calculated using an ellipsoid assumption

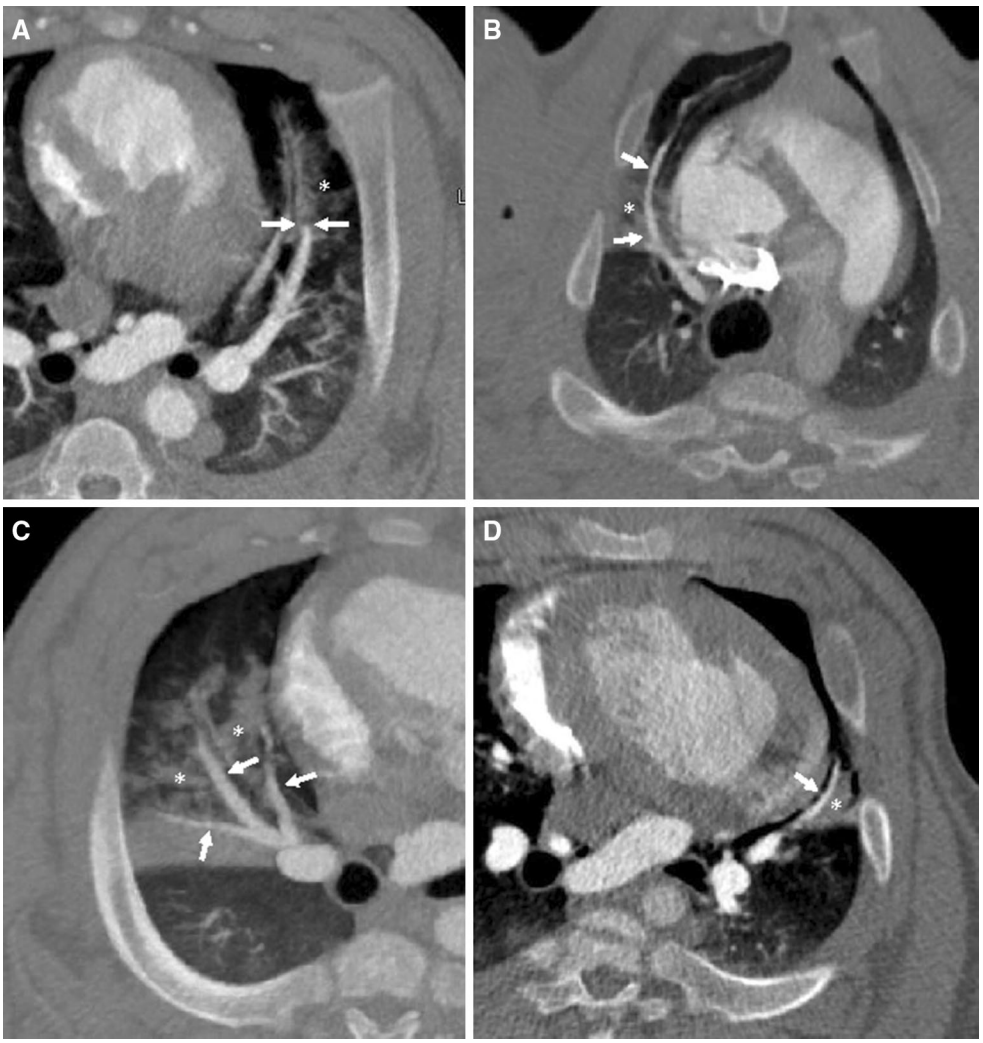

Fig. 2 Examples of pulmonary artery CT measurements. Curved multiplanar maximum intensity projection CTA images demonstrating an occluded pulmonary artery (**A**, *arrows*), a patent pulmonary artery (**B**, *arrows*), multiple adjacent pulmonary artery branches (**C**, *arrows*) and a single pulmonary artery measuring <3 mm in diameter in the ablation zone (**D**, *arrows*). *Asterisks* indicate the ground glass opacity from the preceding microwave ablation. Note that in **A**, the diameter of the occluded vessel was measured just proximal to the site of vessel nonopacification (*arrows*)

versus multiple pulmonary arteries, and those ablation zones that contained a vessel <3 versus ≥3 mm in diameter. A two-tailed unpaired *t* test was also used to compare the mean volume of the ablation zones at CT and gross pathological analysis, and to compare the mean distance between emission point and pulmonary artery branches <3 mm in size. A p value <0.05 was considered statistically significant.

Results

Twenty-one pulmonary microwave ablations were performed in 8 swine. Twelve (57%) ablations were performed in the right lung and 9 (43%) ablations in the left lung. A total of 45 branch pulmonary arteries ≥2 mm in diameter were identified within the 21 ablation zones on post-ablation CT pulmonary angiogram. Six (29%) of the ablation zones contained at least 1 occluded pulmonary artery branch (Fig. 2A). The mean maximum diameter of the occluded pulmonary arteries was 2.4 mm (range: 2–2.8 mm). The mean maximum diameter of the non-occluded pulmonary arteries was significantly larger, measuring 3.7 mm (range: 2.1–6.9 mm; $p = 0.009$; Fig. 2B).

Seven of the 21 (33%) pulmonary arteries measuring less than 3 mm in diameter in the pulmonary ablation zones were occluded, whereas no pulmonary arteries ≥3 mm were occluded (Fig. 4). The mean distance between the emission point of the antenna from the occluded and the non-occluded vessels <3 mm in diameter

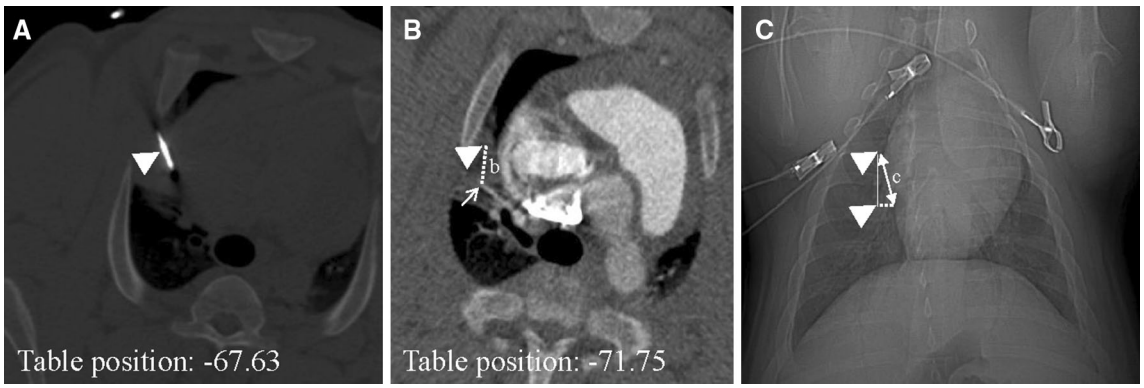

Fig. 3 Triangulation method to determine distance between emission point and occluded pulmonary artery. The emission point of the antenna is identified on post-ablation CT imaging (**A**, *arrowhead*). The cursor on the PACS workstation is then held stationary as the axial images are scrolled through along the craniocaudal axis to identify the axial level of the pulmonary artery occlusion (**B**, *arrowhead*). The difference in CT table position equals the length of *triangle* side "*a*." Next, the distance between the stationary point on the craniocaudal axis (**B**, *arrowhead*) is measured to the site of the vessel occlusion along the transverse plane (occluded artery = *arrow*), providing the length of triangle side "*b*" (*dotted line*). Applying the Pythagorean Theorem, "*c*" equals the closest distance between emission point and the pulmonary artery occlusion. A scout image (**C**) depicts the relationship of the points (*vertical solid line* = "*a*"; *dotted line* = "*b*"; *arrows* = the hypotenuse, "*c*")

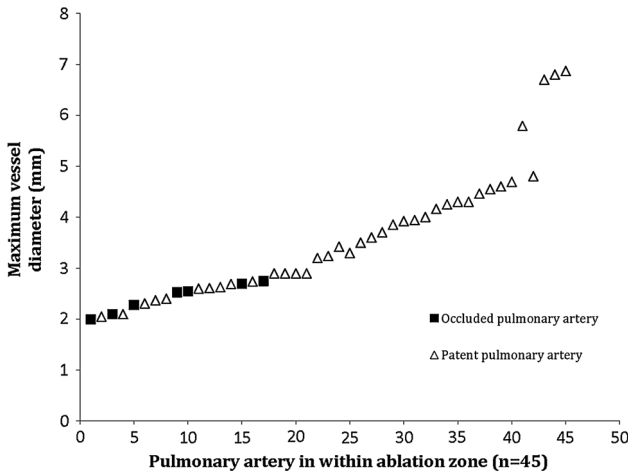

Fig. 4 Graph of branch pulmonary arteries in ablation zones by size and patency. No pulmonary artery occlusions occurred in vessels ≥3 mm in diameter

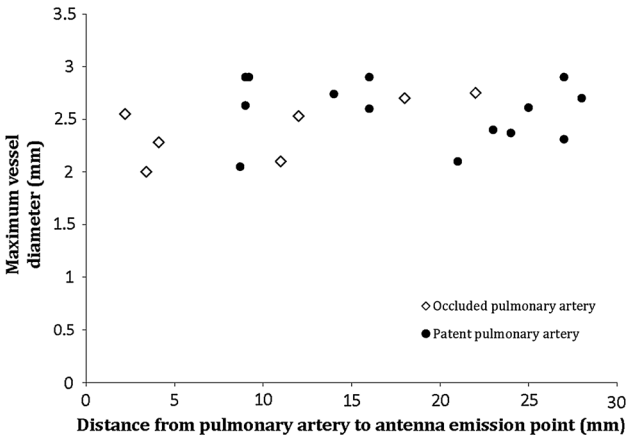

Fig. 5 Scatter gram of branch pulmonary arteries 2–3 mm in size by distance to antenna emission point and patency. No association could be found between distance to emission point and risk of occlusion for vessels of this size

was 16.4 ± 8 mm and 18.1 ± 7 mm, respectively ($p = 0.629$; Fig. 5).

The mean volume of the ablation zones at post-ablation CT and gross evaluation was not significantly different, measuring 13.8 ± 7 and 16.4 ± 4.3 mL, respectively ($p = 0.169$). There was no significant difference in the gross volume of the ablation zones that contained occluded versus non-occluded pulmonary artery branches ($p = 0.42$; Table 1; Fig. 2A), that contained one versus multiple pulmonary artery branches ($p = 0.71$; Table 2; Fig. 2C), or that contained a pulmonary artery measuring <3 versus ≥ 3 mm in diameter ($p = 0.44$; Table 3; Fig. 2D). The mean maximum diameter of the pulmonary ablation zones at CT was also no different across these groups (Tables 1, 2, 3).

No pulmonary artery occlusions remote from the ablation zone occurred nor was there evidence of pulmonary infarction. No partial occlusions of the pulmonary arteries were identified. No immediate post-ablation pseudoaneurysm occurred. There was no large pulmonary hemorrhage at CT or gross pathology.

Discussion

The primary objective of this study was to determine the size of pulmonary artery at risk for occlusion during percutaneous microwave ablation. Therefore, the ablations were intentionally performed in the central lungs where arteries tend to be larger and where an iatrogenic

Table 1 Volumes and maximum diameters of ablation zones containing a ≥1 occluded pulmonary artery versus no occluded pulmonary artery within the ablation zone

	≥1 occluded pulmonary artery in ablation zone $n = 6$	No occluded pulmonary artery in ablation zone $n = 15$	p
Gross ablation zone volume (mL)	17.5 ± 4	15.9 ± 5	0.42
Mean maximum ablation zone diameter at CT (mm)	25.7 ± 5	29.2 ± 5	0.15

Table 2 Volumes and maximum diameters of ablation zones containing a >1 pulmonary artery versus 1 pulmonary artery within the ablation zone

	>1 pulmonary artery in ablation zone $n = 15$	1 pulmonary artery in ablation zone $n = 6$	P
Gross ablation zone volume (mL)	15.6 ± 4	16.4 ± 5	0.71
Mean maximum ablation zone diameter at CT (mm)	28.7 ± 5	30.2 ± 6	0.62

Table 3 Volumes and maximum diameters of ablation zones containing a pulmonary artery <3 versus ≥3 mm in diameter within the ablation zone

	Pulmonary artery <3 mm in ablation zone $n = 3$	Pulmonary artery ≥3 mm in ablation zone $n = 18$	p
Gross ablation zone volume (mL)	17.7 ± 6	15.5 ± 4	0.44
Mean maximum ablation zone diameter at CT (mm)	30.8 ± 5	29.7 ± 6	0.79

pulmonary artery occlusion may theoretically have higher clinical significance. We found that no pulmonary artery branches with a maximum diameter ≥3 mm within the pulmonary ablation zone were occluded and that 30% of pulmonary artery branches 2–3 mm in diameter were occluded on the post-ablation CT pulmonary angiogram. A secondary objective was to determine whether an occluded pulmonary artery, multiple adjacent pulmonary artery branches, or the presence of arteries >3 mm in diameter affected the volume of the resultant pulmonary ablation zone in order to evaluate the effect of vascular heat sink in the lung which may limit ablation zone size. We found no difference in ablation zone volumes among these groups.

Our findings suggest that the degree of blood flow through medium and large size branch pulmonary arteries (>3 mm in diameter) is sufficient to prevent occlusion during a microwave lung ablation for which a common power–time protocol is used. The incidence of pulmonary artery occlusion among smaller vessels (2–3 mm in diameter) was not related to distance from the emission point of the antenna, although the few positive events in this group may have provided insufficient power to demonstrate statistical significance.

Although we could not evaluate the patency of smaller pulmonary arteries (<2 mm in size) due to the spatial resolution limits of CT, a prior study evaluating microwave ablation in rabbit lung found that >90% of vessels with diameters 0.3–2 mm in size were completely thrombosed at histologic evaluation [19]. Thus, a threshold diameter of approximately 2–3 mm seems to exist with microwave pulmonary ablation, above which pulmonary artery branches are resistant to thrombosis as a function of their increased blood flow.

Steinke et al. [13] performed open radiofrequency ablation in sheep to study the vessel size associated with iatrogenic injury. Our results are similar to theirs in that they found a threshold vessel size of approximately 2–4 mm, beyond which vessel thrombosis was rare. However, when comparing the degree of small vessel thrombosis, Steinke found that approximately 20% of vessels <3 mm in size were thrombosed. Similarly, in their comparison of microwave and radiofrequency in rabbit lung, Crocetti et al. [19] also found an approximately 20% thrombosis rate in vessels <2 mm following radiofrequency ablation but a small vessel thrombosis rate of >90% following microwave ablation. These findings

suggest that while the rate of occlusion of large pulmonary blood vessels is similar between radiofrequency and microwave ablation, the rate of small vessel occlusion is higher with microwave ablation. This difference may be attributable to the larger zone of active heating and hotter temperatures generated by microwave ablation and as a result of the impaired electrical conductivity of aerated lung which limits radiofrequency ablation [23]. Microwave energy's relative resistance to local heat sink may be supported by clinical findings from Vogl et al. and Egashira et al. [24, 25] who found that proximity of a tumor to a large blood vessel was not associated with tumor recurrence following pulmonary microwave ablation while proximity to large blood vessels has been identified as a risk factor for local recurrence in prior radiofrequency ablation studies [10, 11].

Despite the ability of medium and large branch pulmonary arteries to remain patent during our study, there was no significant difference in ablation zone volume regardless of whether the ablation zone encompassed a multiple adjacent pulmonary artery branches, arteries >3 mm in diameter, or occluded pulmonary arteries. These findings further support the observations described earlier that pulmonary ablation performed with microwave energy has the ability to overcome local vascular heat sink and generate ablation zones that are reproducible in size.

The diameter of a blood vessel is not the only factor that influences vascular heat sink and predicts frequency of occlusion. Other factors such as blood pressure, velocity, and pulsatility likely contribute to risk of vessel occlusion, as indicated by a recent study evaluating the frequency of hepatic vessel occlusion following microwave ablation which found that portal veins <3 mm in diameter occlude more frequently than hepatic arteries or veins of similar size for this reason [26]. However, direct comparison with medium and large artery diameter and frequency of occlusion in organs other than the lungs is limited by differences in tissue perfusion (likely higher in liver than lung) and by the added effect of ventilation in the lung which has been shown to have a significant effect on heat sink and ablation zone size [7, 9]. As the CT pulmonary angiogram was not timed to evaluate the patency of the pulmonary veins or bronchial arteries in our study, we could not correlate risk of occlusion of these vessels based on vessel diameter but this topic may be an area for future research.

These findings may have several clinical implications. First, our results show it is difficult to cause a medium or large pulmonary artery occlusion with microwave ablation while applying the power and time protocol we used. Thus, a lung tumor abutting a central pulmonary artery may be approached with the intent to fully eradicate the tumor without risk of acute vascular occlusion. The lack of peripheral emboli remote from the central pulmonary ablations also suggests that local endothelial injury and inflammation generated by an adjacent lung ablation does not result in acute peripheral thromboembolism. Second, the ability or inability to occlude a 2- to 3-mm artery in the lung does not significantly change the volume of the resultant microwave ablation zone. If a larger ablation zone is needed, either increasing the microwave power or time, or adding an additional antenna, may be necessary. Pulmonary artery and bronchial occlusion techniques [7–9] may also increase ablation zone volume but have limited clinical data to support them. One theoretical technique to increase ablation zone size with any thermal ablation may be to partly collapse the lung with an artificial pneumothorax to reduce the heat sink from ventilation (which would also shunt blood away and simultaneously reduce perfusion). Lastly, an operator may not need to anticipate a smaller ablation zone size if a microwave antenna is positioned in a region of the lung next to multiple pulmonary artery branches; the ablation zone size appears unaffected by heat sink from the vessels.

There were limitations to this study. First, a single microwave antenna was powered at a set level and for a specific period of time. The use of multiple antennas, antennas from different manufacturers, and the application of higher power and longer ablation time protocols were not tested and may yield different results. Second, these data were acquired from ablations in lungs of healthy swine so the potential carryover to tumors treated in humans with chronic lung disease is not yet known. Third, the patency of the branch pulmonary arteries was assessed only in the immediate post-ablation period. Whether an artery occludes in the subacute to chronic phase or that post-ablation vasospasm resulting in a false positive at CT pulmonary angiography resolves, was not determined. Similarly, the study was not designed to evaluate for subacute or chronic development of pseudoaneurysms.

In summary, we found pulmonary arteries ≥ 3 mm in maximum diameter have a low risk of iatrogenic occlusion during microwave lung ablation with use of a standard ablation protocol. Additionally, ablation zone volumes do not appear to be influenced by the number, diameter or patency of adjacent pulmonary artery branches.

Acknowledgements This study was funded in part by National Institutes of Health Grant R01 CA149379 and by the RSNA Research and Education Foundation, Fellow Research Grant. The authors wish to acknowledge veterinary technician Lisa Sampson, BS for her commitment to ensuring ethical care during the animal experiments.

Compliance with Ethical Standards

Conflict of interest George A. Carberry, Elisabetta Nocerino, Mircea M. Cristescu and Amanda R. Smolock declare that they have no conflict of interests. Fred T. Lee Jr. and Christopher L. Brace are paid consultants for NeuWave Medical, Inc.

References

1. Lencioni R, Crocetti L, Cioni R, et al. Response to radiofrequency ablation of pulmonary tumours: a prospective, intention-to-treat, multicentre clinical trial (the RAPTURE study). Lancet Oncol. 2008;9:621–8.
2. Lanuti M, Sharma A, Digumarthy SR, et al. Radiofrequency ablation for treatment of medically inoperable stage I non–small cell lung cancer. J Thorac Cardiovasc Surg. 2009;137:160–6.
3. Wolf FJ, Grand DJ, Machan JT, DiPetrillo TA, Mayo-Smith WW, Dupuy DE. Microwave ablation of lung malignancies: effectiveness, CT findings, and safety in 50 patients. Radiology. 2008;247:871–9.
4. de Baère T, Risse O, Kuoch V, et al. Adverse events during radiofrequency treatment of 582 hepatic tumors. Am J Roentgenol. 2003;181:695–700.
5. Sakurai J, Mimura H, Gobara H, Hiraki T, Kanazawa S. Pulmonary artery pseudoaneurysm related to radiofrequency ablation of lung tumor. Cardiovasc Intervent Radiol. 2010;33:413–6.
6. Yamakado K, et al. Massive hemoptysis from pulmonary artery pseudoaneurysm caused by lung radiofrequency ablation successful treatment by coil embolization. Cardiovasc Intervent Radiol. 2010;33:410–2.
7. Anai H, et al. Effects of blood flow and/or ventilation restriction on radiofrequency coagulation size in the lung: an experimental study in swine. Cardiovasc Intervent Radiol. 2006;29(5):838–45.
8. Hiraki T, et al. Radiofrequency ablation of normal lungs after pulmonary artery embolization with use of degradable starch microspheres: results in a porcine model. J Vasc Interv Radiol. 2006;17(2):1991–8.
9. Oshima F, et al. Lung radiofrequency ablation with and without bronchial occlusion: experimental study in porcine lungs. J Vasc Interv Radiol. 2004;15(12):1451–6.
10. Iguchi T, Hiraki T, Gobara H, Mimura H, Fujiwara H, Tajiri N, et al. Percutaneous radiofrequency ablation of lung tumors close to the heart or aorta: evaluation of safety and effectiveness. J Vasc Interv Radiol. 2007;18(6):733–40.
11. Hiraki T, et al. Repeat radiofrequency ablation for local progression of lung tumors: does it have a role in local tumor control? J Vasc Interv Radiol. 2008;19(5):706–11.
12. Steinke K, et al. Effect of vessel diameter on the creation of ovine lung radiofrequency lesions in vivo: preliminary results. J Surg Res. 2005;124(1):85–91.
13. Yashiro H, et al. Factors affecting local progression after percutaneous cryoablation of lung tumors. J Vasc Interv Radiol. 2013;24(6):813–21.
14. Brace CL, et al. Pulmonary thermal ablation: Comparison of radiofrequency and microwave devices by using gross pathologic and CT findings in a swine model. Radiology. 2009;251(3):705–11.
15. Andreano A, et al. Microwaves create larger ablations than radiofrequency when controlled for power in ex vivo tissue. Med Phys. 2010;37(6):2967–73.
16. Wright AS, et al. Radiofrequency versus microwave ablation in a hepatic porcine model. Radiology. 2005;236(1):132–9.
17. Nam CY, et al. Microwave liver ablation: influence of hepatic vein size on heat-sink effect in a porcine model. J Vasc Interv Radiol. 2008;19(7):1087–92.
18. Laeseke PF, et al. Microwave ablation versus radiofrequency ablation in the kidney: high-power triaxial antennas create larger ablation zones than similarly sized internally cooled electrodes. J Vasc Interv Radiol. 2009;20(9):1224–9.
19. Crocetti L, et al. Thermal ablation of lung tissue: in vivo experimental comparison of microwave and radiofrequency. Cardiovasc Intervent Radiol. 2010;33(4):818–27.
20. Care IoLARCo, Animals UoL, Resources NIoHDoR. Guide for the care and use of laboratory animals.: National Academies; 1985.
21. Yamamoto A, Nakamura K, Matsuoka T, et al. Radiofrequency ablation in a porcine lung model: correlation between CT and histopathologic findings. Am J Roentgenol. 2005;185:1299–306.
22. Goldberg SN, Gazelle GS, Compton CC, McLoud TC. Radiofrequency tissue ablation in the rabbit lung: efficacy and complications. Acad Radiol. 1995;2:776–84.
23. Brace CL. Radiofrequency and microwave ablation of the liver, lung, kidney, and bone: what are the differences? Curr Probl Diagn Radiol. 2009;38(3):135–43.
24. Vogl TJ, et al. Factors influencing local tumor control in patients with neoplastic pulmonary nodules treated with microwave ablation: a risk-factor analysis. Am J Roentgenol. 2013;200(3):665–72.
25. Egashira Y, Singh S, Bandula S, Illing R. Percutaneous high-energy microwave ablation for the treatment of pulmonary tumors: a retrospective single-center experience. J Vasc Interv Radiol. 2016;27(4):474–9.
26. Chiang J, Cristescu M, Lee M, et al. Vascular occlusion during microwave ablation of hepatocellular carcinomas. Radiology. 2016;281(2):617–24.